Colloids and Surfaces A: Physicochemical and Engineering Aspects 732 (2026) 139168

Contents lists available at ScienceDirect

Colloids and Surfaces A: Physicochemical and Engineering Aspects

journal homepage: www.elsevier.com/locate/colsurfa

Tuning the wetting properties of Paraloid B72 from hydrophilicity to superamphiphobicity combined with antibacterial properties

Panagiotis N. Manoudis [a], Ioannis Zuburtikudis [b], Styliani Permathouli [c], Avraam Konstantinidis [d], Hadil Abu Khalifeh [b], Christine Kottaridi [c], Ioannis Karapanagiotis [e,*]

[a] Lysis Consulting P.C., Thessaloniki 55534, Greece
[b] Department of Chemical Engineering, Abu Dhabi University (ADU), P.O. Box 59911, Abu Dhabi, United Arab Emirates
[c] School of Biology, Aristotle University of Thessaloniki, Thessaloniki 54124, Greece
[d] School of Civil Engineering, Aristotle University of Thessaloniki, Thessaloniki 54124, Greece
[e] School of Chemistry, Aristotle University of Thessaloniki, Thessaloniki 54124, Greece

GRAPHICAL ABSTRACT

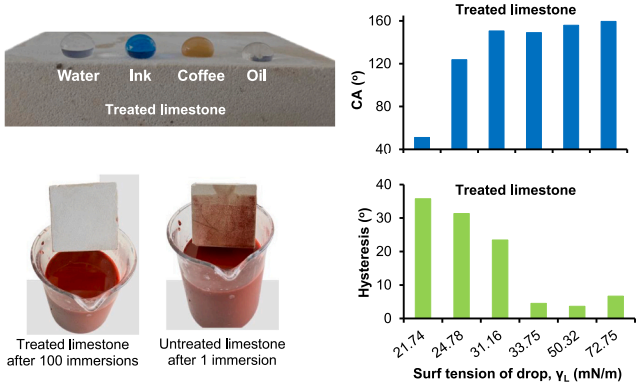

ARTICLE INFO

Keywords:
Superamphiphobic
Superhydrophobic
Superoleophobic
Antibacterial
Paraloid
Stone
Cultural heritage

ABSTRACT

Paraloid B72 is a methyl acrylate/ethyl methacrylate copolymer which is extensively used as a consolidant, binder, adhesive, protective coating and varnish for the conservation and preservation of cultural heritage buildings and objects. In this study, a one-step method is developed to convert the inherently hydrophilic B72 into a superamphiphobic material, thereby improving its protective performance against both water- and oil-based pollutants. In particular, B72 is blended with silica nanoparticles (Si) and a fluororesin (F) in various concentrations, producing coatings which are initially deposited on glass (reference substrate). The nanoparticles highly affect the surface morphology of the coatings, inducing superhydrophobicity, whereas F lowers its apparent surface energy resulting to superamphiphobicity. A systematic study is conducted to carefully select the relative concentrations of the two additives, Si and F, which are necessary to achieve the desired superamphiphobicity. The interaction of the selected superamphiphobic coating with liquid drops spanning a wide

* Corresponding author.
E-mail address: karapana@chem.auth.gr (I. Karapanagiotis).

https://doi.org/10.1016/j.colsurfa.2025.139168
Received 2 September 2025; Received in revised form 8 November 2025; Accepted 3 December 2025
Available online 4 December 2025

range of surface tensions is examined, while the evaporation process of a water drop on the superamphiphobic surface is shown to be governed by a series of stick-slip events. Furthermore, it is demonstrated that the coating imparts superamphiphobicity to wood, paper, cotton and limestone. The latter is subjected to further investigations, revealing that the treatment has minimal impact on both the colour and breathability of limestone while it enhances the resistance of the treated stone to capillary water absorption. Finally, a key finding is that the liquid-repellent nature of the superamphiphobic coating inhibits the growth of *S. aureus*.

1. Introduction

Paraloid B72 consistently draws significant attention from the scientific community, as it is a versatile material extensively used for the conservation of heritage buildings made of natural stone and other objects of the cultural heritage [1–5]. As B72 is an organic polymer it has faced considerable criticism, particularly for its incompatibility with inorganic materials [6,7]. Despite these concerns, B72 is still widely used in conservation practice and therefore continues to be a material of ongoing research, as evidenced by the plethora of relative published articles. Overall, B72 is appreciated for its mechanical properties and ease of use [8]. Moreover, it demonstrates good thermal stability [9] and resistance to UV radiation [10,11], although under prolonged exposure it may undergo significant degradation [12,13].

B72 is a methyl acrylate/ethyl methacrylate (MA/EMA) copolymer with a low amount of butyl methacrylate (BMA) units [14]. To improve the properties of the acrylate polymers designed for the protection and conservation of cultural heritage, two approaches were followed. First, acrylate polymers were modified by introducing fluorine atoms to their structures, thus producing fluorinated acrylate-based resins with enhanced hydrophobicity, resistance to the UV radiation and overall improved efficacy and durability [15–21].

In the second approach, nanoparticles (NPs) were incorporated into acrylate polymers, including B72, to impart improved properties to the resulting composite/hybrid materials. For instance, titanium dioxide (TiO_2) NPs were incorporated into B72 to induce photocatalytic self-cleaning properties [22,23]. Zinc oxide (ZnO) [24,25] and zinc titanium oxide ($ZnTiO_3$) [24] NPs were dispersed in the B72 matrix to develop hybrid materials with enhanced properties, including biocidal activity. Additionally, calcium carbonate ($CaCO_3$) NPs, which are chemically compatible with calcareous stones, were blended with an acrylate copolymer (MA/EMA) of similar composition to B72 [26].

The second approach, that involves the use of NPs, was adopted to produce B72-based hybrid materials of enhanced hydrophobicity or even superhydrophobicity. The latter is defined by a static contact angle of water drops larger than 150° (CA_W>150°) and a very small contact angle hysteresis of water drops (CAH_W<10°) which implies small sliding angle (SA_W<10°). It is stressed that, for practical applications, the dynamic contact angles (CAH_W, SA_W) are more important than the static contact angle (CA_W), as their low values govern the water repellency and the rolling motion of water drops (lotus effect) [27]. Notably, certain rare surfaces, such as the rose petal, exhibit high CA_W, yet also display high CAH_W and SA_W, making them water-adhesive rather than water-repellent surfaces [28]. As water plays a significant role in various direct and indirect degradation processes of heritage materials, producing superhydrophobic, lotus-like materials for the protection of cultural heritage is very important, as described in several review articles [29–31]. However, the majority of the superhydrophobic materials developed for the protection of cultural heritage are composites of siloxane-based polymers combined with NPs. Only few attempts have been made to induce superhydrophobicity or enhanced hydrophobicity in acrylate polymers, particularly in B72, as summarized in Table 1 and described next.

D'Amato et al. incorporated TiO_2 and silicon dioxide (SiO_2) NPs into B72 and obtained a CA_W of up to 135° [32]. In a more systematic method, Ntelia and Karapanagiotis produced a composite coating, comprising B72 and hydrophilic SiO_2 NPs, which exhibited superhydrophocity with high CA_W (>150°) and low SA_W (<15°) [33]. As both B72 and SiO_2 are inherently hydrophilic materials, the study demonstrated that superhydrophobicity can be achieved through appropriate surface design, without the need for chemical modification involving low surface energy compounds, as suggested in other reports [34–36]. The composite coating had a minimal impact on the colour of treated marble or wood, while it noticeably altered the color of brass [33]. Additionally, the coating exhibited good chemical stability [33]. The method was further elaborated by He et al. who mixed B72 and hydrophobic SiO_2 NPs, achieving extreme non-wetting properties on treated paper, fabric, and wood, with CA_W> 160° and SA_W< 10° [37]. The colours of treated substrates were not affected by the application of the composite coating and air permeability was maintained [37]. Zhou et al. enriched the above recipe by adding polydimethylsiloxane (PDMS) to the B72 and hydrophobic nano-SiO_2 [38]. The hybrid coating was deposited on mural surfaces which exhibited remarkable superhydrophobic properties. The inclusion of PDMS significantly enhanced water repellency, as evidenced by the exceptional SA_W, with the lowest reported value being approximately 5°. Moreover, the coating maintained minimal impact on the murals' color and breathability, alongside other advantageous characteristics [38]. In another attempt, SiO_2 NPs were first functionalised with hexamethyldisilazane (HMDS) and then incorporated into a blend of B72 and fluorinated polymers [39]. The resulting composite material was deposited on bricks which obtained enhanced hydrophobicity with a CA_W up to 142° and resistivity against weathering from acid, alkali, salt and UV radiation [39]. Bai et al. wrapped TiO_2 with a SiO_2 shell which was functionalised by grafting methyl (Me) groups [40]. The obtained TiO_2@Si–Me core-shell NPs showed superhydrophobicity. The superhydrophobic NPs were incorporated into B72 solution and the dispersion was deposited on marble which obtained enhanced hydrophobicity with 145°<CA_W< 150° [40].

The aim of this study is to tailor the wetting properties of B72 by incorporating SiO_2 NPs and a fluorosilane resin, in order to develop a superamphiphobic hybrid coating capable of repelling virtually any liquid with a surface tension between that of water (~72 mN/m) and oil (~32 mN/m). Superamphiphobic coatings can be highly beneficial to protect heritage buildings and objects, particularly in urban environments where oil-based pollutants pose significant threats. Despite their potential, only a few studies have developed and investigated superamphiphobic, liquid-repellent coatings for cultural heritage conservation, and these have relied on silane-based systems rather than acrylate polymers [41–44]. To the best of our knowledge, this is the first attempt to produce a superamphiphobic B72-based coating. Equally important is the finding of the present study that the superamphiphobic nature of the

Table 1
NPs and other polymers added to Paraloid B72 to promote hydrophobicity. The reported contact (CA_W) and sliding (SA_W) angles of water drops are included.

NP	Other polymer	CA_W	SA_W	Ref
SiO_2 & TiO_2 (hydrophilic)	-	~135°	n.r.	[32]
SiO_2 (hydrophilic)	-	> 150°	< 15°	[33]
SiO_2 (hydrophobic)	-	> 160°	< 10°	[37]
SiO_2 (hydrophobic)	PDMS	> 160°	< 10°	[38]
SiO_2 (functionalized with HMDS)	Fluorinated polymers	> 140°	n.r.	[39]
TiO_2@Si–Me (superhydrophobic)	-	> 145°	n.r.	[40]

n.r.=not reported.

produced coating inhibits the growth of bacteria, such as *S. aureus*, without using a biocidal agent.

The investigation is carried out in three phases. First, a super-amphiphobic B72-based coating is developed through the careful selection of NP and fluororesin concentrations (Section 3.1). In this phase, experiments are conducted using glass slides as substrates, because glass surface is atomically smooth and has minimal influence on the morphology and, therefore, the wetting properties of the deposited coatings [30]. Second, since B72 is widely used for treating various materials, the versatility of the developed coating to induce super-amphiphobicity to different substrates is demonstrated (Section 3.2). Finally, the focus shifts to limestone, a material extensively used in both heritage and modern buildings (Section 3.3). It is shown that coated limestone samples exhibit two important properties: extreme liquid (water and oil) repellency and antibacterial properties.

2. Experimental

2.1. Materials

Paraloid B72 and acetone were purchased from In Situ (Greece) while hydrophobic pyrogenic silica nanoparticles (HDK®H30RM) with a high specific surface area (~ 200 m^2/g) were provided by Wacker (Germany). SRA-450, a fluorochemical resin concentrate in ethyl acetate, was purchased from 3 M (USA). According to the manufacturer the product contains 40 % w/w active solids. Drops of distilled water, sunflower oil (purchased from the local market) and isopropanol (obtained from Sisco Research Laboratories, India) were used to study the wetting properties of the coating surfaces. Aqueous hydrochloric acid solution (HCl) and sodium hydroxide (NaOH) were purchased from Penta Chemicals (Czech Republic) and were used to prepare drops of different pH. Limestone specimens originating from Crete, Greece were obtained from K-Stones (Greece). Other materials, used as substrates such as glass, balsa wood, paper, kraft paper white and brown cotton were obtained from the local market. For the antimicrobial test sterile petri dishes and Nutrient broth (Panreac Applichem, Spain, reference CA413793.1210) were used.

2.2. Coating preparation and characterisation

Paraloid B72 was dissolved in acetone to prepare a stock solution of 3 % w/w. Silica nanoparticles (NPs) were dispersed in Paraloid solutions in various concentrations i.e. 0.5, 1.0, 2.0 and 3.0 % w/w. The dispersions were stirred vigorously for 20 min at ambient conditions and were cast (2 mL) onto clean glass slides using a pipette. For comparison, solution of pure Paraloid (without NPs) was also deposited onto glass.

Dispersions of B72 and 2 % w/w NPs were enriched with the fluororesin at concentrations of 0.2, 0.4, 0.8, and 1.2 % w/w. These concentrations correspond to the active solids of the SRA-450 product. The dispersions were then deposited onto glass slides following the previously described procedure. Moreover, dispersions containing B72, 2 % w/w NPs and 1.2 % w/w fluororesin were prepared and deposited onto sandstone, balsa wood, paper, kraft paper white and brown cotton. The produced coating is referred to as B72-2Si-1.2F.

Contact angles (CAs) of drops of various liquids and contact angle hystereses (CAHs) were measured in triplicate using the ImageJ software. At least three drops were placed on different areas of coated glass samples and average values were calculated. Scanning electron microscopy (SEM; TM3000, Hitachi, Japan) was employed to study surface morphologies of the deposited coatings. Surface roughness measurements were carried out using a confocal microscope (Leica DCM8, Leica Microsystems CMS, Germany) at profilometer mode.

To evaluate the performance of the B72-2Si-1.2F coating for the protection of limestone, some more experiments were conducted as follows. Water absorption by capillarity and water vapour permeability experiments were conducted on limestone samples coated with B72-2Si-1.2F. For comparison, the same tests were also performed on samples coated with B72 (reference). For the capillary water absorption test, pre-weighed, coated limestone samples were placed in a vessel containing distilled water, with the coated side facing downward, and kept under ambient conditions for 24 h. After this period, the samples were gently wiped to remove surface-adhered water and then re-weighed. For the water vapour permeability test, limestone blocks were mounted with the coated surface facing upward on top of polypropylene containers half-filled with distilled water. The blocks were sealed onto the containers using a reusable adhesive (Blu Tack), and the entire assembly was wrapped laterally with parafilm, leaving only the treated surface exposed to the surrounding air. The assemblies were then placed in a thermostatic cabinet maintained at 40 °C. Each setup was weighed every 24 h until the weight difference between two consecutive measurements was less than 2 %. The above-described procedures were followed using pristine (uncoated) limestone specimens.

The stability of the B72-2Si-1.2F coating on limestone against the effects of the UV radiation was tested using a chamber equipped with a 300-W Osram Ultra Vitalux light (UV-A component). The tested samples were exposed to the extreme UV conditions for 24 h. A thermal imaging camera (UTi 120MS, UNI-Trend Technology, China) was used to estimate the temperature of the samples during UV exposure. Drops with pH ranging from 0 to 14 were placed on the surfaces of treated limestone samples and CAs were measured. The solutions were prepared using hydrochloric acid (HCl, ChemLab) and sodium hydroxide (NaOH, ChemLab). Finally, the anti-smudge performance of the B72-2Si-1.2F coating was demonstrated by repeatedly dipping a coated limestone sample into a water–mud bath 100 times.

Antimicrobial testing was conducted using the gram-positive *Staphylococcus aureus* (NCIMB #8625). Bacterial strains were grown in autoclaved nutrient broth medium. Uncoated limestone and limestone samples with B72 and B72–2Si-1.2F coatings were placed individually into sterilised containers, and 400 μL of each bacterial culture was applied to the surface of each sample. The specimens were incubated overnight at room temperature in a humid, saturated environment. The next day, both samples and the attached membranes were rinsed with 10 mL of autoclaved 0.9 % NaCl with continuous agitation for 30 min. The resulting suspensions were subjected to serial tenfold dilutions, which were plated onto nutrient agar Petri dishes and incubated overnight at 37°C. Post-incubation, colony-forming units per millilitre (cfu/mL) were determined for each condition. The antimicrobial efficacy of each coating was assessed by comparing the recovered bacterial counts against the uncoated limestone sample. All experiments were performed with technical replicates to ensure reproducibility and reliability of the results.

3. Results and discussion

3.1. Method development: from hydrophilicity to superhydrophobicity and superamphiphobicity

The wetting properties of coatings prepared using B72 and varying silica nanoparticle (NP) concentration are investigated in Fig. 1**a**. The water contact angle (CA_W) increases with NP concentration rising from 74.8° (pure B72) to values exceeding the threshold of superhydrophobicity (CA_W>150°) when the NP concentration reaches 2 % or 3 % w/w. Conversely, the water contact angle hysteresis (CAH_W) decreases with NP concentration, dropping from 63.6° (pure B72) to values below 10° at 2 % or 3 % w/w NP concentration. The origin of the CAH_W variation, reported in Fig. 1**a**, is revealed in Fig. 1**b** which shows the variations of the advancing (ACA_W) and receding (RCA_W) contact angles of water drops. Both ACA_W and RCA_W increase with NP concentration but not with the same rate. RCA_W rises significantly faster than ACA_W leading to a reduction of CAH_W (=ACA_W–RCA_W) as NP concentration increases.

The behaviours of CA_W and CAH_W discussed above, align with

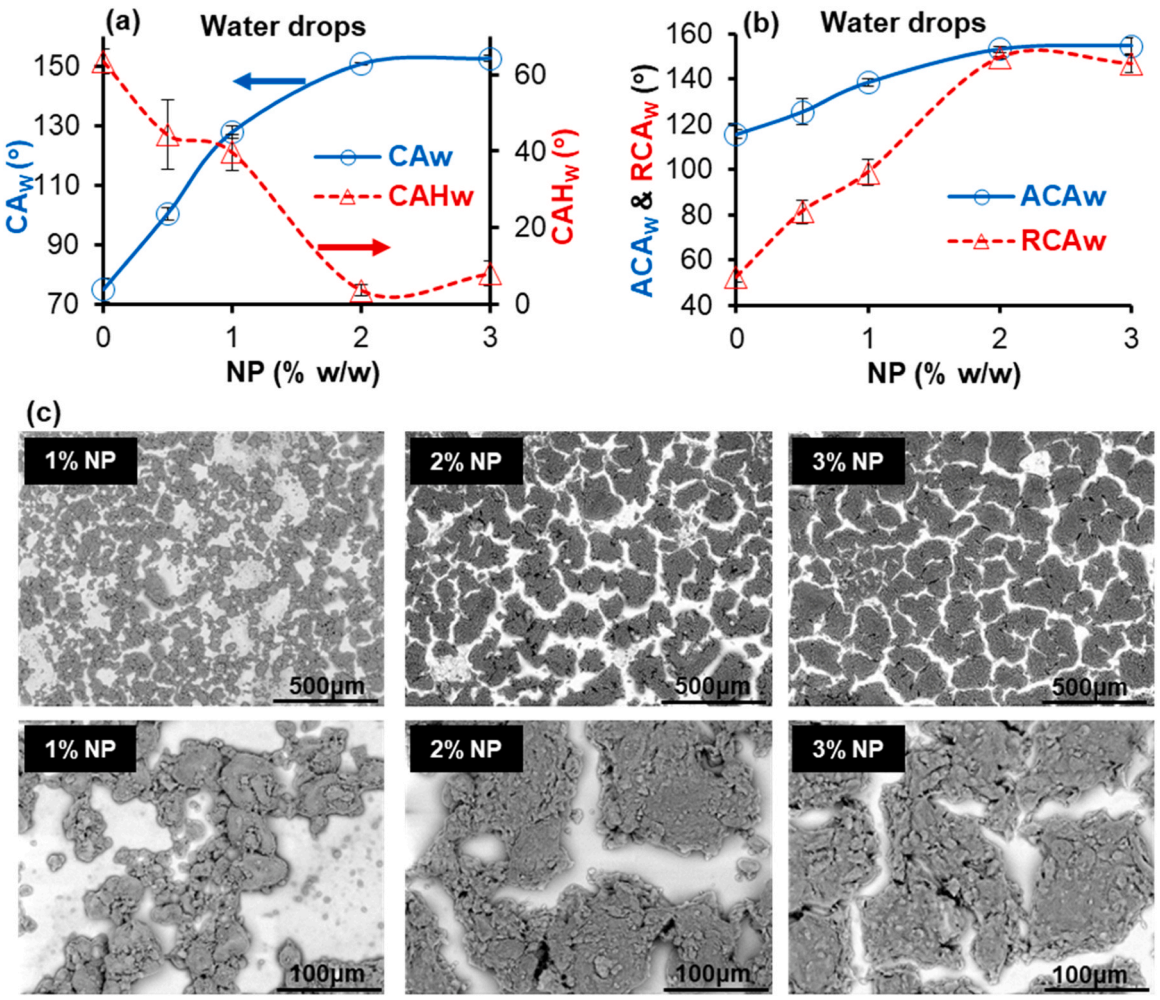

Fig. 1. (a) Contact angle (CA_W) and contact angle hysteresis (CAH_W) of water drops vs the silica NP concentration. (b) Advancing (ACA_W) and receding (RCA_W) contact angles of water drops vs the silica NP concentration. (c) SEM images at low (top) and high (bottom) magnifications of coating surfaces prepared with 1 %, 2 %, and 3 % w/w silica NPs, as indicated. All coatings were applied to glass substrates.

previously published studies on the effect of silica NP concentration on the wetting properties of B72-silica composite coatings. These studies reported that CA_W increases while CAH_W decreases with rising NP concentration, with superhydrophobicity and water repellency achieved at high NP concentrations [33,37,38]. The evolution of the observed non-wetting properties is attributed to the influence of the NPs on the surface morphology of the polymer–NP composite coatings, as evidenced by the SEM images in Fig. 1**c** and revealed in previous studies [30,33,41,42,44]. At lower NP concentrations (e.g., 1 % w/w), discrete microscale clusters are formed, interspersed with relatively smooth areas. As the NP concentration increases to 2 % and 3 % w/w, these clusters grow in size and begin to coalesce, resulting in a densely textured surface that underlies the observed superhydrophobicity and water repellency [30,33,41,42,44].

According to the results of Fig. 1, either the NP concentration of 2 or 3 % w/w could be selected for further consideration, as they provide comparable levels of the desired superhydrophobicity and water repellency. Between these two concentrations, the lower one (i.e., 2 % w/w) is selected to prepare coatings for further studies in order to align with the ongoing concern about the potential toxic effects of NPs [45,46]. Moreover, the mechanical stability of the composite coating is expected to deteriorate as the NP concentration increases [31].

The selected composite coating, consisting of B72 and 2 % w/w NP (hereafter referred to as B72–2Si) demonstrated oleophilicity, as the contact angle of oil drops (CA_O) was only 56.5°. Therefore, it was clear that in order to achieve oleophobicity, it was necessary to add a low surface energy agent to the B72–2Si formulation. Fig. 2 reveals the effect of the concentration of the fluororesin which was added to B72–2Si coatings. The results suggest that the fluororesin had practically no effect on the interaction of water drops with the coating surface, as both CA_W and CAH_W are stable in the plots of Figs. 2**a** and 2**b**, respectively. Therefore, superhydrophobicity and water repellency were maintained for any tested fluororesin concentration. However, adding fluororesin to coating's formulation led to a major increase in the contact angle of oil drops (CA_O) and a significant reduction of the corresponding contact angle hysteresis (CAH_O). At the fluororesin concentration of 1.2 % w/w a very high CA_O (=149.6°) and a very low CAH_O (=4.5°) were measured. In sum, the composite coating, consisting of B72, 2 % w/w NP and 1.2 % w/w fluororesin (hereafter referred to as B72-2Si-1.2F) can be considered superamphiphobic, as it is capable to repel both water and oil. It is noted that the advancing and receding contact angles of water (ACA_W and RCA_W) and oil (ACA_O and RCA_O) drops, which were used to calculate the hystereses (CAH_W and CAH_o) in Fig. 2, are provided in Figure S1 of the Supplementary file.

Fig. 3**a** illustrates the variation of the fractions of coating surfaces (f_s) in contact with water drops as a function of NP and fluororesin concentrations. Specifically, the figure highlights the effects of incorporating NPs into B72 (B72 based coatings) and the impact of adding fluororesin to B72–2Si (B72–2Si based coatings). The f_s parameter, which reflects surface morphology, is included in the Cassie-Baxter

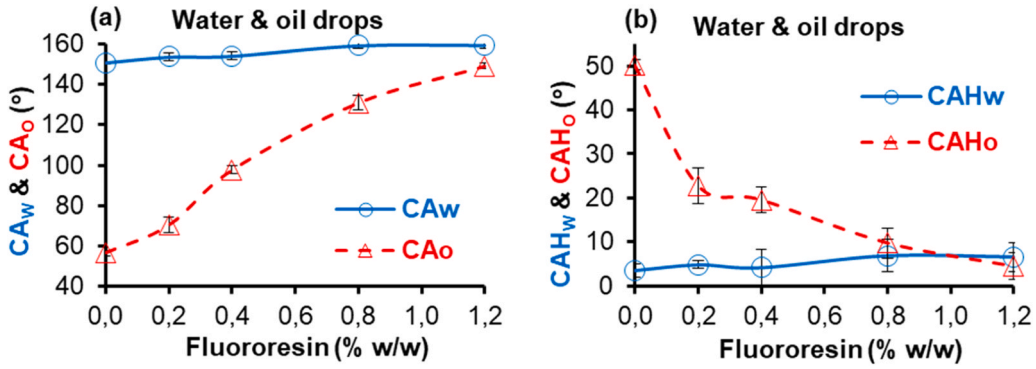

Fig. 2. (a) Contact angle of water (CA_W) and oil (CA_O) drops vs the concentration of the fluororesin which was added to B72–2Si coatings. (b) Contact angle hysteresis of water (CAH_W) and oil (CAH_o) drops vs the concentration of the fluororesin which was added to B72–2Si coatings. Glass was used as substrate for coating deposition.

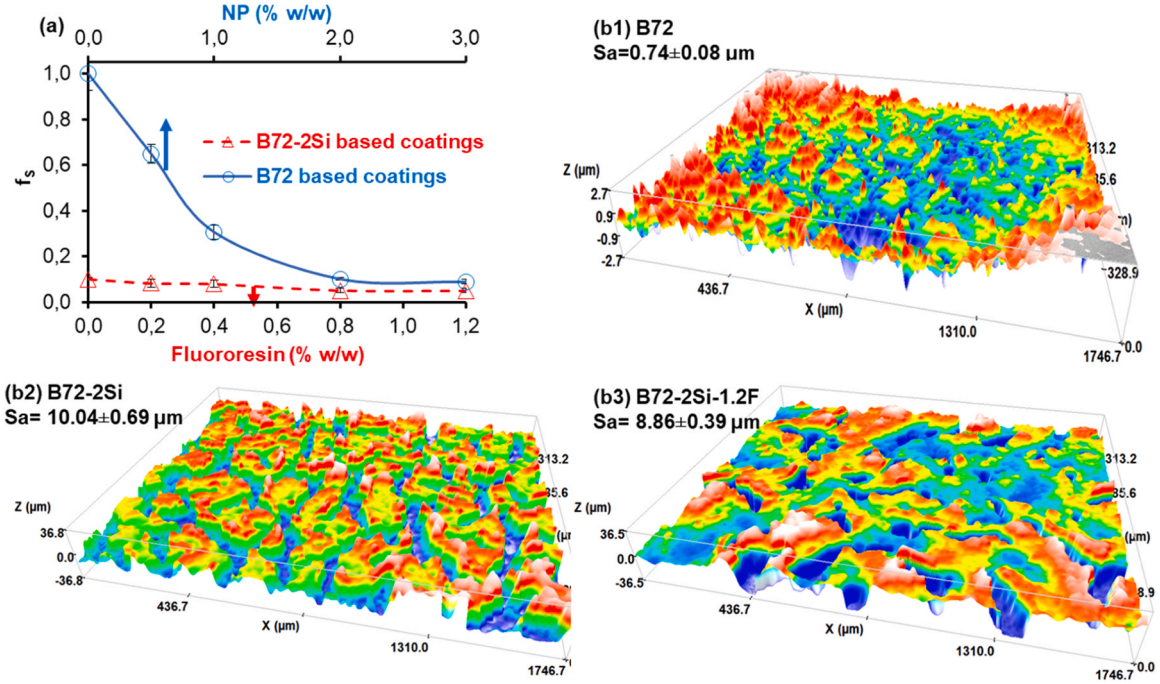

Fig. 3. (a) Variation of the solid fraction (f_s) contacted by the water droplet as a function of NP and fluororesin concentrations. (b) Profilometry images and roughness measurements taken from the surfaces of the following coatings on glass: pure B72 (b1), B72–2Si (b2) and B72-2Si-1.2F (b3).

equation to relate the water contact angle on a rough surface (θ_R) to that on a smooth surface (θ_s) [47]:

$$\cos\theta_R = -1 + f_s(\cos\theta_s + 1) \quad (1)$$

Using the CA_W values reported in Figs. 1**a** and 2**a** for θ_R in Eq. 1 and taking $\theta_s = 74.8°$ which was measured for water drops on smooth B72 surface, the f_s values were calculated and the results are reported in Fig. 3**a**. The results for the B72 based coatings show that adding NPs to B72 has an enormous effect on f_s which is reduced from 1.00 (smooth B72 coating) to 0.10 (rough B72–2Si coating). However, the incorporation of the fluororesin into B72–2Si based coatings, had a smaller effect, reducing f_s from 0.10 (B72–2Si coating) to only 0.05 (B72-2Si-1.2F coating). Notably, similarly low f_s values have been reported in previous studies which investigated the surface structures of superhydrophobic surfaces, suggesting a very low fraction of the textured solid being in contact with the water drop [48–51].

The dominant influence of NPs and the comparatively minor effect of fluororesin on the surface morphology of the coatings are confirmed by surface roughness measurements, which are listed in the typical profilometry images of Fig. 3**b**. The average surface roughness (Sa) of the smooth B72 coating is 0.74 ± 0.08 μm, increasing by over one order of magnitude (Sa=10.04 ± 0.69 μm) for the B72–2Si coating. This finding aligns with the significant reduction of f_s, caused by the NPs, which was reported for the B72–2Si based coatings in Fig. 3**a**. Moreover, the measured increase in surface roughness with the addition of NPs indicates that the Cassie–Baxter model should be applied (as was done) to interpret the results in Fig. 1**a**. Since B72 is inherently hydrophilic, with a contact angle of $CA_W = 74.8°$ (<90°), the results cannot be explained by the Wenzel model [52], which predicts that surface roughness amplifies the intrinsic hydrophilic or hydrophobic character of a material. Instead, the wettability results in Fig. 1**a** are consistent with the Cassie–Baxter model, which suggests that the CA_W of any material (whether inherently hydrophilic or hydrophobic) increases with surface roughness.

As shown in Fig. 3b, the Sa for the B72-2Si-1.2F coating was measured to be 8.86 ± 0.39 μm. Consequently, according to the profilometry measurements the B72-2Si-1.2F coating is slightly smoother than the B72–2Si coating (Sa=10.04 ± 0.69 μm). However, it is

important to note that the difference in surface roughness between the two composite coatings is minimal, when considering the standard deviations in the Sa measurements, thus confirming that the fluororesin has only a minor effect on surface roughness. Moreover, it is noteworthy that the slightly smoother B72-2Si-1.2F coating corresponds to a lower f_s (=0.05) compared to the slightly rougher B72–2Si (f_s=0.10). This highlights that the contact area of the drop with the coating surface is influenced not only by the surface structure but also by its chemical composition.

To further discuss the effect of the fluororesin on the wettability of the produced coatings two more calculations were conducted. First, the forces (F) per unit length that cause water and oil drops to move along the surfaces of the B72–2Si based coatings, were calculated using the following equation [53,54]:

$$F = \gamma_L(\cos\theta_R - \cos\theta_A) \quad (2)$$

where θ_R and θ_A are the receding (RCA) and advancing (ACA) contact angles and γ_L is the surface tension of the liquid, taken as γ_L= 72.75 mN/m for the water drops and γ_L= 33.75 mN/m for the (sunflower) oil drops [55]. Taking into account the values of ACA(=θ_A) and RCA(=θ_R) which are provided in Figures S1a (for water drops) and **S1b** (for oil drops), the forces F_W (water drops) and F_O (oil drops) were calculated using Eq. 2, across varying fluororesin concentration. The results are provided in Fig. 4**a** and show that F_O decreases significantly with the fluororesin concentration whereas F_W remains practically unaffected. In summary, Fig. 4**a** demonstrates that the fluororesin greatly enhances oil repellency but has practically no effect on the water repellent character of the B72–2Si based coatings.

In the second set of calculations, the Chibowski equation was used to assess the apparent surface energies of the B72–2Si based coatings (γ_s) using the ACA(=θ_A) and RCA(=θ_R) values of water drops (Figure S1a) [56]:

$$\gamma_s = \frac{\gamma_L(1+\cos\theta_A)^2}{2+\cos\theta_R+\cos\theta_A} \quad (3)$$

The results are presented in Fig. 4**b** and indicate that γ_s decreases as the fluororesin concentration increases. Specifically, γ_s decreases from 3.5 mJ/m^2 for the superhydrophobic B72–2Si coating to 1.3 mJ/m^2 for the superamphiphobic B72-2Si-1.2F coating. These calculated values are consistent with previously reported data for other liquid-repellent surfaces [57,58].

Based on the results reported so far, the B72-2Si-1.2F coating is selected for further studies due to its superamphiphobic properties, demonstrating extreme repellency against both water and oil. To gain deeper insight into its interaction with liquids, two additional experiments were conducted. First, the wetting properties of the B72-2Si-1.2F coating were further examined using drops of water and isopropanol (IPA) mixtures, which cover a fairly wide range of surface tension (γ_L) values depending on the water-to-IPA mass ratio, as detailed in Table S1 of the Supplementary file [59]. The results for the CA and CAH of these drops are shown in Figs. 5**a** and 5**b**, respectively. In addition, results for drops of pure IPA as well as pure water (CA_W and CAH_W) and oil (CA_O and CAH_O) drops are also included in Fig. 5. The results indicate that CA increases while CAH decreases with the liquid surface tension (γ_L). The transition to extreme non-wetting, falls within the critical range of 31–34 mJ/m^2. The drop with γ_L= 31.16 mJ/m^2 exhibits a large CA of 150.7°. However, this drop does not roll off the surface easily as CAH is still relatively high (=23.4°). The (oil) drop with a slightly higher γ_L (=33.75 mJ/m^2) demonstrates both large CA (>150°) and small CAH (<10°). The extreme non-wetting properties are maintained for drops with γ_L above the critical range.

In the second experiment, a water drop was placed on the B72-2Si-1.2F coating and allowed to evaporate under ambient conditions. The evolutions of CA_W and the liquid-solid apparent contact diameter (d), normalized to its initial value (do), were monitored during the evaporation process. The results are provided in Fig. 6 and show that the evaporation process is dominated by a series of stick-slip events. Four "sticky" regions are identified in the plot of Fig. 6, where the contact diameter remains nearly constant, indicating that evaporation follows the constant contact radius (CCR) mode. These "sticky" regions are separated by five slip events. At the start of each slip event, the contact line depins, abruptly shifting to a smaller value before becoming pinned again, maintaining a constant contact diameter until the next slip occurs. This stick-slip evaporation behavior has been previously observed on superhydrophobic surfaces [41,60].

3.2. Application of the superamphiphobic coating on various substrates

As described in the Introduction, Paraloid B72 is used for the protection and preservation of a wide range of materials and objects. Therefore, a brief study was conducted to assess the applicability of the developed superamphiphobic B72–2Si-1.2F coating on different substrates, which correspond to a large variety of applications ranging from cultural heritage to paper and textile industry. Kraft paper was included in the tested substrates, as a particular interest has been recently emerged to induce extreme non-wetting properties to this type of paper, which is used by the packaging industry [61]. The results are provided in Table 2 which shows measurements of static and dynamic contact angles of water and oil drops on coated substrates, as well as colour changes induced by the coating applications. Notably, colourimetric results are particularly important for assessing the performance of materials

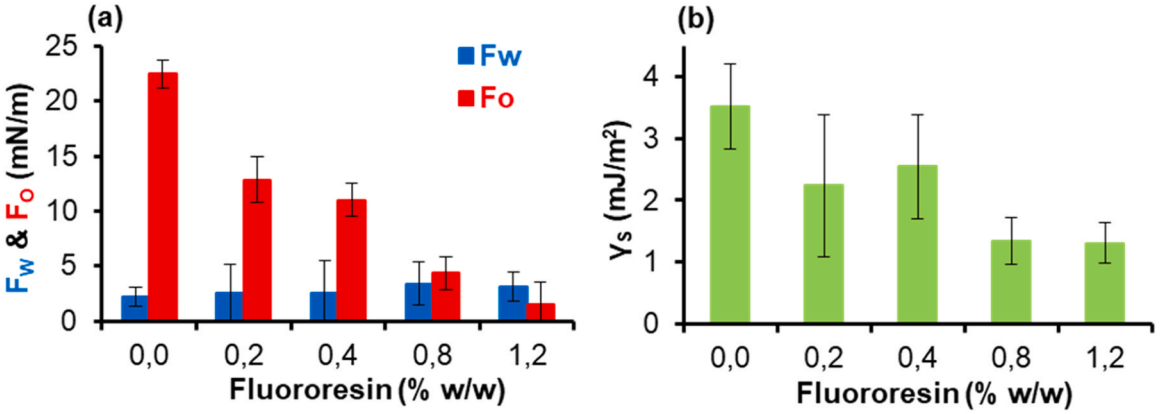

Fig. 4. (a) Force per unit length that causes water (F_W) and oil (F_O) drops to move along the surfaces of the B72–2Si based coatings vs the concentration of the fluororesin. Calculations were performed using Eq. 2. (b) Apparent surface energies (γ_s) of B72–2Si based coatings, calculated using Eq. 3, vs the concentration of the fluororesin. Coatings were deposited on glass.

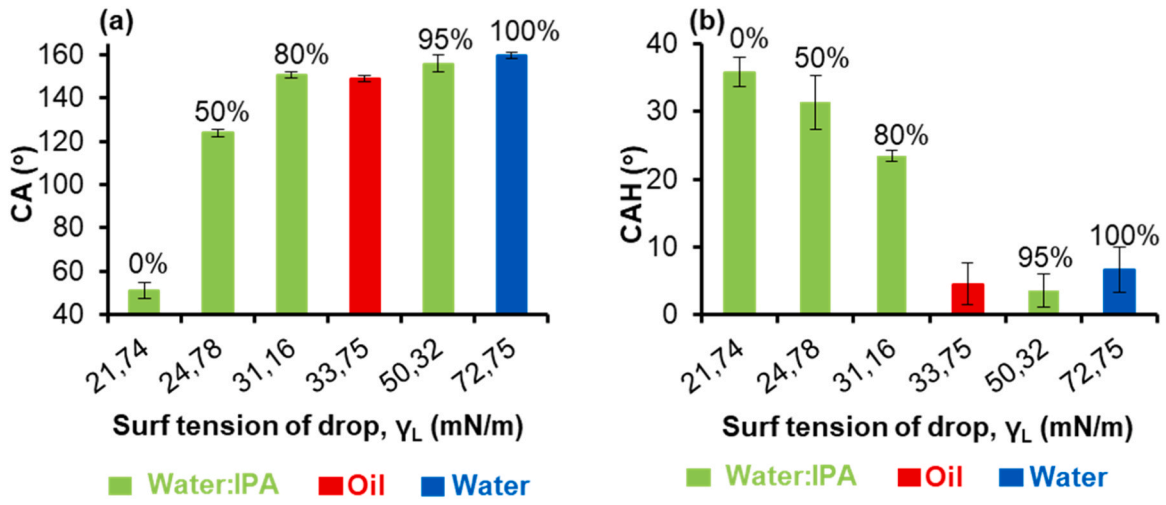

Fig. 5. (a) CA and CAH of liquid drops on B72-2Si-1.2F coatings vs the surface tension of the liquid (γ_L) drop. The concentrations of water (% w/w) in the mixtures are included in the plots and correspond to 50, 80 and 95 % w/w. In addition, results for drops of pure IPA (i.e. 0 % water), pure water (i.e. no IPA) and oil are included in the plots. Values for pure water (CA_W & CAH_W) and oil (CA_O & CAH_O) were reproduced from Figs. 2**a** and 2**b**. Coatings were deposited on glass.

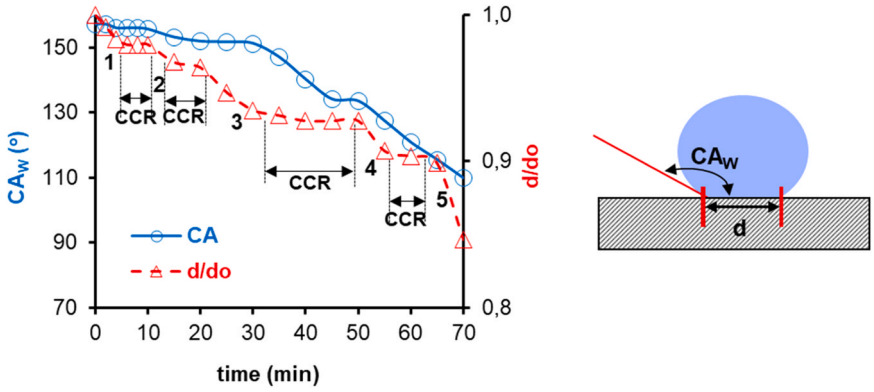

Fig. 6. CA_W and contact diameter (d) normalised to its initial value (do) vs evaporation time for a water drop which was placed on a B72-2Si-1.2F coating. Five slip events (1−5) are identified, which are separated by regions where d remains nearly constant, indicating that evaporation in these "sticky" regions is dominated by the constant contact radius (CCR) mode. Glass was used as substrate for the deposition of the B72-2Si-1.2F coating.

Table 2
Wetting properties and colour change (ΔE) of various substrates, treated with the superamphiphobic B72-2Si-1.2F coating.

Substrate	CA_W (°)	CAH_W (°)	CA_O (°)	CAH_O (°)	ΔE
Limestone	160.2 ± 0.4	3.5 ± 1.4	146.9 ± 1.2	6.8 ± 1.2	3.1 ± 1.0
Balsa wood	160.3 ± 0.9	6.9 ± 1.0	147.6 ± 0.7	5.1 ± 2.5	4.2 ± 0.5
Paper	158.4 ± 0.8	6.6 ± 0.3	149.9 ± 1.2	8.6 ± 3.8	1.0 ± 0.2
Kraft paper	159.3 ± 0.6	4.3 ± 1.1	147.6 ± 0.7	6.9 ± 1.9	7.2 ± 0.5
White cotton	160.2 ± 0.3	5.7 ± 1.0	149.7 ± 3.5	8.3 ± 1.2	1.2 ± 0.3
Brown cotton	159.5 ± 0.8	4.2 ± 1.7	147.3 ± 0.9	9.2 ± 1.9	28.1 ± 1.9

intended for cultural heritage conservation, as significant colour changes in pristine materials are unacceptable in heritage science. The total colour variations (ΔE) of the coated samples, compared to the pristine (uncoated) samples, were calculated using the following equation:

$$\Delta E = \sqrt{\Delta L^{*2} + \Delta a^{*2} + \Delta b^{*2}} \quad (4)$$

where ΔL^*, Δa^* and Δb^* are the changes of the lightness, the red–green component and the yellow–blue component of the CIE 1976 scale, respectively, which are defined as follows: $\Delta L^* = L^*_c - L^*_u$; $\Delta a^* = a^*_c - a^*_u$; $\Delta a^* = b^*_c - b^*_u$. The "c" and "u" subscripts indicate the coated and uncoated samples, respectively.

According to the results presented in Table 2, superamphiphobicity was achieved on all coated substrates, as evidenced by the high contact angles and low contact angle hysteresis values. Specifically, for every substrate listed in Table 2 it is reported that $CA_W > 155°$ and $CA_O > 145°$ while $CAH_W < 7°$ and $CAH_O < 10°$. Examples of water and oil drops on bare and coated limestone and cotton are shown in the photographs Figure S2. The advancing and receding contact angles used to calculate the hysteresis values reported in Table 2 are provided in Figure S3.

The colour changes (ΔE) reported in Table 2 are generally below 5, with the exception of kraft paper ($\Delta E = 7.2$) and brown cotton ($\Delta E = 28.1$). Notably, any ΔE value below 5 is typically considered minor and acceptable within the conservation practices of cultural heritage [62]. The variations of the ΔE results are elucidated if we take into consideration the values of the L^*, a^* and b^* coordinates which are given in Figure S4 of the Supplementary file.

According to Figure S4, the application of the B72-2Si-1.2F coating

caused virtually no change in the colour coordinates for paper and white cotton, resulting in ΔE values below 1.5 (Table 2). In the cases of limestone and balsa wood, the coating led to notable reductions in the a^* and b^* values (Figure S4), which corresponded to moderate colour changes, with ΔE values of 3.1 and 4.2, respectively (Table 2). For kraft paper, the decreases in a^* and b^* were even more pronounced (Figure S4), leading to a higher overall colour change of 7.2 (Table 2). As shown in Figure S4, the application of the B72-2Si-1.2F coating resulted in significant changes in the colour coordinates of brown cotton, marked by a pronounced increase in L^* and substantial decreases in both a^* and b^*. As silica NPs are whitish their application on brown, dark cotton resulted in a major enhancement of brightness/lightness and this was reflected in the rise of the L^* value. Moreover, the NPs shifted the a^* and b^* values to substantially lower values, as indicated in Figure S4. Consequently, the overall colour change (ΔE) for brown cotton was as high as 28.1 (Table 2). Brown cotton was deliberately included among the tested substrates to deliver the message that the B72-2Si-1.2F coating is not suitable for the treatment of dark-coloured materials, whenever the preservation of the original colour of the substrate is important, as it is in the case of cultural heritage conservation.

3.3. *Evaluation of the superamphiphobic coating for the protection of limestone*

According to the results of Table 2, the B72–2Si-1.2F coating induced superamphiphobicity to limestone while it caused only moderate change to the colour of the pristine stone which is within the acceptable limits of conservation practice i.e., $\Delta E = 3.1 < 5$. The exceptional non-wetting behaviour of limestone specimens treated with the superamphiphobic coating is illustrated in the photographs of Fig. 7. Specifically, Fig. 7**a** displays static drops of water, water-based ink, coffee and oil on the coated limestone surface. Fig. 7**b** shows water and oil drops sliding off the surface of tilted, coated specimens. The self-cleaning capability is depicted in the successive snapshots of Fig. 7**c**, where methylene blue particles, which were deliberately placed on the surface of coated limestone, are effectively removed by rolling water drops.

To assess the protective performance of the B72-2Si-1.2F coating on limestone against prolonged exposure to liquid water, the relative reduction of water absorption by capillarity (RC%) was calculated using the following equation:

$$RC\% = \frac{m_{uw} - m_{cw}}{m_{uw}} \times 100 \quad (5)$$

where m_{uw} and m_{cw} are the masses of water absorbed by capillarity per unit area, by the uncoated and coated limestone samples, respectively. The effect of the B72-2Si-1.2F coating on the breathability of limestone was evaluated by calculating the relative reduction of water vapour permeability (RVP%) using the following equation:

$$RVP\% = \left(\frac{m_{uv} - m_{cv}}{m_{uv}}\right) \times 100 \quad (6)$$

where m_{uv} and m_{cv} are the masses of water vapour per unit area which penetrate the uncoated and coated limestone samples, respectively.

The effects of the B72-2Si-1.2F coating on the capillary water absorption and vapour permeability are revealed by the results of Table 3. For comparison, the RC% and the RVP% were calculated for limestone samples coated with B72 (reference). The results for the water absorption test show that the composite coating (RC% = 48) provided more than twice (RC% = 22) the level of protection compared to the reference B72 coating (Table 3). It is worth noting that the limited effectiveness of B72 in reducing water absorption by capillarity has also been

Table 3
Relative reductions of water absorption by capillarity (RC%) and vapour permeability (RVP%) for limestone samples treated with B72 and B72-2Si-1.2F coatings.

Coating	RC%	RVP%
B72	22	17
B72-2Si-1.2F	48	6

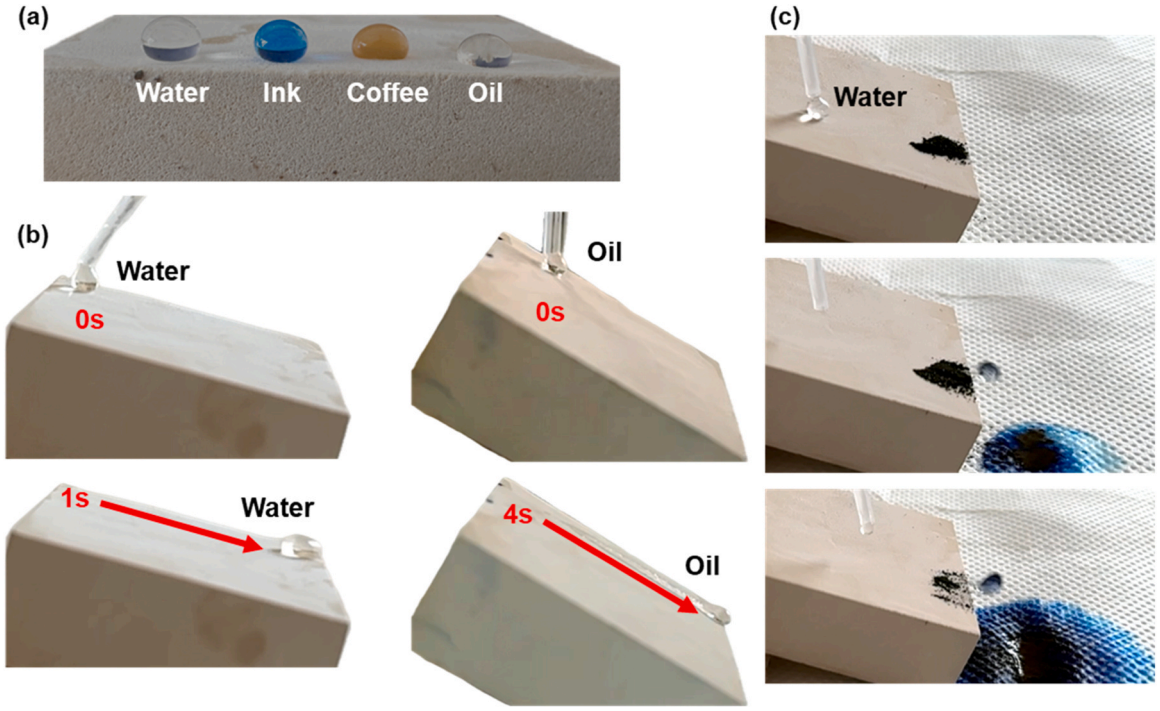

Fig. 7. Photographs demonstrating the non-wetting properties of limestone specimens, treated with the B72-2Si-1.2F coating. (a) Drops of liquids on the surface of coated limestone. (b) Water and oil drops sliding down the inclined, coated limestone. (c) Demonstration of the self-cleaning effect, as water drops remove contaminants from the coated limestone surface.

highlighted in previous studies [7,38].

Furthermore, the results presented in Table 3 indicate that the application of the composite coating was beneficial in terms of vapour permeability when compared to the B72 coating. The limestone sample treated with B72 exhibited an RVP% of 17, whereas the sample treated with the composite, superamphiphobic coating showed a significantly lower RVP% of 6. This finding aligns with previously published studies, which have demonstrated that the diffusion rate of water vapour through porous materials increases as the hydrophobicity of the pores is enhanced, due to the suppression of water molecule condensation [63–66]. In particular, experiments conducted on calcareous stones and marble have shown that water vapour diffuses more readily through hydrophobic pores than through hydrophilic ones [64–66]. Thus, the reduced RVP% observed for the sample treated with the superamphiphobic composite coating, compared to the hydrophobic B72-coated sample, is consistent with the aforementioned literature [63–66]. Finally, it is noted that the RVP% of 17, reported in Table 3 for limestone coated with B72 is in agreement with the RVP% of 16.3 reported by Zhou et al. for mural crafts treated with the same acrylate i.e., B72 [38].

The stability of the B72-2Si-1.2F coating against the UV radiation is revealed in Fig. 8a1 and 8a2 which show that the CAs (Fig. 8**a1**) and CAHs (Fig. 8a2) of both water and oil drops on the B72-2Si-1.2F coating were practically unaffected by the accelerated ageing treatment. Only a slight increase of CAH_O be noticed which, however, is almost within the experimental error. Notably, a side effect of the UV radiation was a significant temperature increase of the sample during treatment, which exceeded approximately 120°C, as evidenced by the thermal image shown in Fig. 8**a3**. Furthermore, colourimetric measurements conducted after the artificially accelerated ageing process revealed a ΔE value of 1.1 ± 0.7. This value, calculated relative to the uncoated limestone which was not exposed to the UV radiation, is notably lower than the ΔE reported in Table 2 ($\Delta E = 3.1 \pm 1.0$) for coated limestone prior to UV exposure. These results suggest that UV treatment significantly affected the appearance of the coated sample, making it more similar to that of the uncoated stone. This change implies partial degradation or possible removal of the coating. However, this alteration did not compromise the coating's non-wetting properties, as evidenced by the data presented in Fig. 8a. The excellent chemical resistance of the B72-2Si-1.2F coating against drops of varying pH is demonstrated in Fig. 8**b**. The composite coating exhibits consistently high CAs and low CAHs across a broad pH range, indicating strong liquid repellency irrespective of the drop's acidity or alkalinity. The anti-smudge performance of the B72-2Si-1.2F coating is demonstrated in Fig. 8**c1**. A limestone sample coated with the composite material was repeatedly dipped into a water-mud bath 100 times, yet the surface remained visibly clean. In contrast, as shown in Fig. 8**c2**, the uncoated limestone surface became heavily soiled after just a single immersion, with mud adhering strongly to the surface. In sum, the results of Fig. 8 indicate that the B72-2Si-1.2F coating exhibits notable stability across the various tests it underwent. However, it should be stressed that long-term exposure of the coating to outdoor environmental conditions is essential in order to draw reliable conclusions about its durability under real-world conditions.

Calcareous stones, such as limestone, are highly vulnerable to bacterial colonization, which can lead to both aesthetic alteration and structural degradation [67]. Hence, the potential antibacterial properties of the B72-2Si-1.2F coating could be a major advantage for the protection of limestone. Typically, the antibacterial efficacy of protective coatings is achieved through the incorporation of biocidal agents such as, for instance, ZnO or TiO_2, into their formulation. Notably, none of these agents were used for the production of the B72-2Si-1.2F. However, as shown in Fig. 9, the application of the superamphiphobic coating on limestone significantly inhibited the growth of *S. aureus*. In particular, Fig. 9 presents the cfu/mL results obtained for uncoated limestone specimens, as well as those coated with B72 and B72-2Si-1.2F. The B72 coating offered considerable protection against bacterial growth, achieving an inhibition of 94.3 %. However, stone protection against the growth *S. aureus* was largely enhanced when the

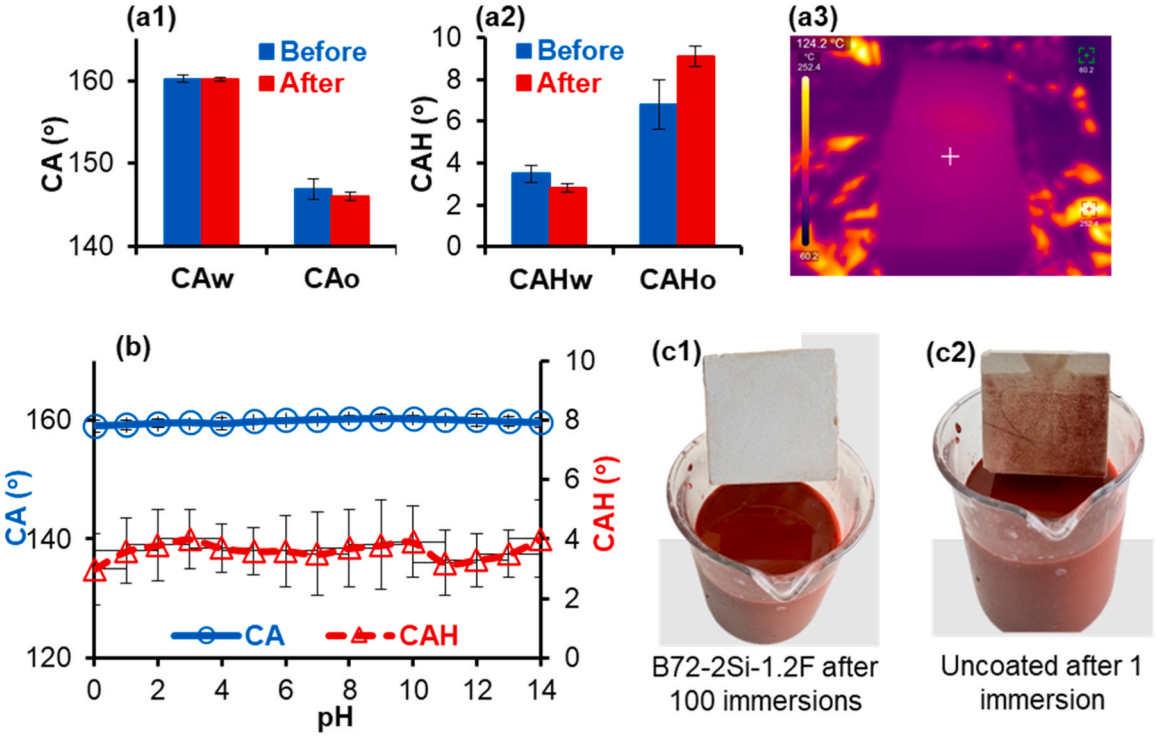

Fig. 8. (a) Stability of the B72-2Si-1.2F coating against the artificially accelerated UV radiation. (a1) CA and (a2) CAH results for water and oil drops on coated limestone samples, before and after UV exposure. (a3) Thermal image captured during the UV exposure process. (b) CA and CAH values of aqueous drops on limestone coated with B72-2Si-1.2F, plotted as a function of drop pH. (c1) The surface of limestone coated with B72-2Si-1.2F remained clean after 100 immersions in a mud bath. (c2) Uncoated limestone became visibly soiled after just one immersion.

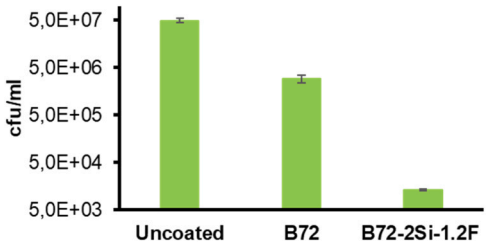

Fig. 9. The cfu/mL results that were retrieved from the uncoated and coated limestone samples which were inoculated with *S. aureus* liquid cultures.

B72-2Si-1.2F coating was used for the treatment of the limestone. According to the results, the cfu/mL values for *S. aureus* retrieved from the B72-2Si-1.2F coated limestone are significantly lower than those from the B72-coated samples, corresponding to an inhibition rate of 99.9 %.

4. Conclusions

The development of a superamphiphobic material based on Paraloid B72 –a methyl acrylate/ethyl methacrylate copolymer widely used in the conservation and preservation of cultural heritage– is reported. The method was initially optimised using glass substrates for the deposition of the various coatings. To modify the inherently hydrophilic nature of the copolymer, a two-step approach was followed. First, B72 was blended with silica (Si) nanoparticles (NPs), which altered the surface morphology of the resulting coatings, leading to superhydrophobicity. Second, a fluororesin (F) was incorporated into the formulation, reducing the apparent surface energy of the coating and ultimately yielding a superamphiphobic coating. Based on studies which revealed the influence of the relative concentrations of Si NPs and F on the wetting properties of the composite coating, it was concluded that the optimal formulation to proceed with was 2 % w/w Si and 1.2 % w/w F, referred to as B72-2Si-1.2F coating. It was found that liquid drops placed on the B72-2Si-1.2F coating, with surface tension values exceeding the critical threshold of 31–34 mN/m, exhibited very high contact angles (i.e., $>150^{\circ}$) and very low contact angle hysteresis (i.e., $<10^{\circ}$). The evaporation process of a water drop on the superamphiphobic B72-2Si-1.2F coating was dominated by a series of stick-slip events. The versatility of the method was demonstrated by showing that the B72-2Si-1.2F coating imparts superamphiphobicity to a variety of substrates, including limestone, wood, paper, kraft paper and cotton. Focusing on limestone it was shown that the B72-2Si-1.2F coating had a minimal impact on both the colour and breathability of natural stone while it significantly enhanced the resistance of the treated stone to capillary water absorption. The coated limestone obtained self-cleaning properties and anti-smudge performance while its repellent properties were practically not affected by the UV radiation or the pH of the drop. It is noted, however, that long-term exposure of coated specimens to atmospheric conditions is important for a more comprehensive evaluation of the coating's durability under real conditions. Finally, it was found that the liquid-repellent nature of the superamphiphobic B72-2Si-1.2F coating induced antibacterial properties as it inhibited the growth of *S. aureus*.

CRediT authorship contribution statement

Hadil Abu Khalifeh: Investigation. **Christine Kottaridi:** Writing – original draft, Supervision, Methodology. **Styliani Permathouli:** Investigation. **Avraam Konstantinidis:** Investigation. **Ioannis Karapanagiotis:** Writing – original draft, Supervision, Methodology, Conceptualization. **Ioannis Zuburtikudis:** Supervision, Funding acquisition. **Manoudis Panagiotis:** Methodology, Investigation.

Declaration of Competing Interest

The authors declare that they have no known competing financial interests or personal relationships that could have appeared to influence the work reported in this paper.

Acknowledgements

The financial support of Abu Dhabi University through the Internal Research, Innovation and Impact Grant No. 19300777 to Ioannis Zuburtikudis is greatly acknowledged.

Appendix A. Supporting information

Supplementary data associated with this article can be found in the online version at doi:10.1016/j.colsurfa.2025.139168.

Data Availability

Data will be made available on request.

References

[1] M. Brugnara, E. Degasperi, C.D. Volpe, D. Maniglio, A. Penati, S. Siboni, L. Toniolo, T. Poli, S. Invernizzi, V. Castelvetro, The application of the contact angle in monument protection: New materials and methods, Colloid Surf. A 241 (2004) 299–312.
[2] M. Favaro, R. Mendichi, F. Ossola, U. Russo, S. Simon, P. Tomasin, P.A. Vigato, Evaluation of polymers for conservation treatments of outdoor exposed stone monuments. Part I: photo-oxidative weathering, Polym. Degrad. Stab. 91 (2006) 3083–3096.
[3] M. Sadat-Shojai, A. Ershad-Langroudi, Polymeric coatings for protection of historic monuments: opportunities and challenges, J. Appl. Polym. Sci. 112 (2009) 2535–2551.
[4] A. Pedna, G. Giuntoli, M. Frediani, P. Frediani, L. Rosi, Synthesis of functionalized polyolefins with novel applications as protective coatings for stone cultural heritage, Prog. Org. Coat. 76 (2013) 1600–1607.
[5] D. Pinna, M. Galeotti, B. Perito, G. Daly, B. Salvadori, In situ long-term monitoring of recolonization by fungi and lichens after innovative and traditional conservative treatments of archaeological stones in Fiesole (Italy), Int. Biodeter. Biodegr. 132 (2018) 49–58.
[6] A. Artesani, F. Di Turo, M. Zucchelli, A. Traviglia, Recent advances in protective coatings for cultural heritage–an overview, Coatings 10 (2020) 217.
[7] G. Masi, A.Dal Pozzo, G. Ugolotti, A. Tugnoli, E. Sassoni, Choosing the consolidant for carbonate substrates: technical performance and environmental sustainability of selected inorganic and organic products, Constr. Build. Mater. 407 (2023) 133599.
[8] Vinçotte, E. Beauvoit, N. Boyard, E. Guilminot, Effect of solvent on Paraloid® B72 and B44 acrylic resins used as adhesives in conservation, Herit. Sci. 7 (2019) 42.
[9] M. Lazzari, O. Chiantore, Thermal-ageing of paraloid acrylic protective polymers, Polymer 41 (2000) 6447–6455.
[10] O. Chiantore, M. Lazzari, Photo-oxidative stability of Paraloid acrylic protective polymers, Polymer 42 (2001) 17–27.
[11] H.V. Farmakalidis, S. Boyatzis, A.M. Douvas, I. Karatasios, S. Sotiropoulou, P. Argitis, Y. Chryssoulakis, V. Kilikoglou, The effect of TiO_2 component on the properties of acrylic and urea-aldehyde resins under accelerated ageing conditions, Pure Appl. Chem. 89 (2017) 1659–1671.
[12] M.J. Melo, S. Bracci, M. Camaiti, O. Chiantore, F. Piacenti, Photodegradation of acrylic resins used in the conservation of stone, Polym. Degrad. Stab. 66 (1999) 23–30.
[13] P. Kotlík, K. Doubravová, J. Horálek, L. Kubáč, J. Akrman, Acrylic copolymer coatings for protection against UV rays, J. Cult. Herit. 15 (2014) 44–48.
[14] O. Chiantore, M. Lazzari, Characterization of acrylic resins, Int. J. Polym. Anal. Charact. 2 (1996) 395–408.
[15] G. Alessandrini, M. Aglietto, V. Castelvetro, F. Ciardelli, R. Peruzzi, L. Toniolo, Comparative evaluation of fluorinated and unfluorinated acrylic copolymers as water-repellent coating materials for stone, J. Appl. Polym. Sci. 76 (2000) 962–977.
[16] V. Castelvetro, M. Aglietto, F. Ciardelli, O. Chiantore, M. Lazzari, L. Toniolo, Structure control, coating properties, and durability of fluorinated acrylic-based polymers, J. Coat. Technol. 74 (2002) 57–66.
[17] L. Toniolo, T. Poli, V. Castelvetro, A. Manariti, O. Chiantore, M. Lazzari, Tailoring new fluorinated acrylic copolymers as protective coatings for marble, J. Cult. Herit. 3 (2002) 309–316.
[18] S.K. Papadopoulou, G. Dritsas, I. Karapanagiotis, I. Zuburtikudis, C. Panayiotou, Surface characterization of poly(2,2,3,3,3-pentafluoropropyl methacrylate) by inverse gas chromatography and contact angle measurements, Eur. Polym. J. 46 (2010) 202–208.

[19] W. Yao, Y. Li, Z. Huang, Fluorinated poly(methyl)acrylate: synthesis and properties, Polymer 55 (2014) 6197–6211.
[20] V. Sabatini, E. Pargoletti, V. Comite, M.A. Ortenzi, P. Fermo, D. Gulotta, G. Cappelletti, Towards novel fluorinated methacrylic coatings for cultural heritage: a combined polymers and surfaces chemistry study, Polymers 11 (2019) 1190.
[21] E. Pargoletti, V. Comite, P. Fermo, V. Sabatini, L. Annunziata, M.A. Ortenzi, H. Farina, G. Cappelletti, Calcitic-based stones protection by a low-fluorine modified methacrylic coating, Environ. Sci. Pollut. Res. Int. 29 (2022) 29455–29466.
[22] M.F. La Russa, N. Rovella, M.A. De Buergo, C.M. Belfiore, A. Pezzino, G.M. Crisci, S.A. Ruffolo, Nano-TiO2 coatings for cultural heritage protection: the role of the binder on hydrophobic and self-cleaning efficacy, Prog. Org. Coat. 91 (2016) 1–8.
[23] G. Giuntoli, M. Bini, B. Ciuffi, B. Salvadori, G. Baldi, L. Rosi, Nanodispersions of TiO_2 in water for removing acrylic films used in conservation, Polymers 13 (2021) 3966.
[24] S.A. Ruffolo, M.F. La Russa, M. Malagodi, C. Oliviero Rossi, A.M. Palermo, G. M. Crisci, ZnO and $ZnTiO_3$ nanopowders for antimicrobial stone coating, Appl. Phys. A 100 (2010) 829–834.
[25] A.-A.T. Traistaru, I.C.A. Sandu, M.C. Timar, G.L. Dumitrescu, I. Sandu, SEM-EDX, water absorption, and wetting capability studies on evaluation of the influence of nano-zinc oxide as additive to Paraloid B72 solutions used for wooden artifacts consolidation, Microsc. Res. Tech. 76 (2013) 209–218.
[26] M.A. Aldoasri, S.S. Darwish, M.A. Adam, N.A. Elmarzugi, S.M. Ahmed, Enhancing the durability of calcareous stone monuments of ancient Egypt using $CaCO_3$ nanoparticles, Sustainability 9 (2017) 1392.
[27] D. Öner, T.J. McCarthy, Ultrahydrophobic surfaces. Effects of topography length scales on wettability, Langmuir 16 (2000) 7777–7782.
[28] L. Feng, Y. Zhang, J. Xi, Y. Zhu, N. Wang, F. Xia, L. Jiang, Petal effect: a superhydrophobic state with high adhesive force, Langmuir 24 (2008) 4114–4119.
[29] Y. Cao, A. Salvini, M. Camaiti, Current status and future prospects of applying bioinspired superhydrophobic materials for conservation of stone artworks, Coatings 10 (2020) 353.
[30] Karapanagiotis, P.N. Manoudis, Superhydrophobic and superamphiphobic materials for the conservation of natural stone: an overview, Constr. Build. Mater. 320 (2022) 126175.
[31] H. Chen, Y. Cao, C. Wang, F. Tie, W. Dong, M. Camaiti, P. Baglioni, Superhydrophobic surfaces for the sustainable maintenance of building materials and stone-built heritage: the challenges, opportunities and perspectives, Adv. Colloid Inter. 335 (2025) 103343.
[32] R. D'Amato, L. Caneve, C. Giancristofaro, F. Persia, L. Pilloni, A. Rinaldi, Development of nanocomposites for conservation of artistic stones, Proc. Inst. Mech. Eng. Part N J. Nanoeng. Nanosyst. 228 (2014) 19–26.
[33] E. Ntelia, I. Karapanagiotis, Superhydrophobic paraloid B72, Prog. Org. Coat. 139 (2020) 105224.
[34] S. Herminghaus, Roughness-induced non-wetting, Eur. Lett. 52 (2000) 165–170.
[35] W. Xiao, Z. Huang, Z. He, Tuning the wettability on La0.7Sr0.3MnO3 coatings from superhydrophilicity to superhydrophobicity by hierarchical microstructure, Appl. Phys. Lett. 89 (2006) 083101.
[36] P.N. Manoudis, I. Karapanagiotis, Modification of the wettability of polymer surfaces using nanoparticles, Prog. Org. Coat. 77 (2014) 331–338.
[37] W. He, J. Ou, F. Wang, S. Lei, X. Fang, W. Li, A. Amirfazli, Transparent and superhydrophobic coating via one-step spraying for cultural relic protection against water and moisture, Colloid Surf. A 662 (2023) 130949.
[38] X. Zhou, W. He, J. Ou, Y. Hu, F. Wang, X. Fang, W. Li, A. Amirfazli, Translucent superhydrophobic coating for murals protection, Colloid Surf. A 689 (2024) 133750.
[39] T. Li, Y. Fan, K. Wang, S. Song, X. Liu, N. Bu, R. Li, Q. Zhen, S. Bashir, Methyl-modified silica hybrid fluorinated Paraloid B-72 as hydrophobic coatings for the conservation of ancient bricks, Constr. Build. Mater. 299 (2021) 123906.
[40] X. Bai, S. Yang, C. Tan, T. Jia, L. Guo, W. Song, M.P. Jian, X. Zhang, Z. Zhang, L. Wu, H. Yang, H. Li, D. Hao, Synthesis of TiO_2 based superhydrophobic coatings for efficient anti-corrosion and self-cleaning on stone building surface, J. Clean. Prod. 380 (2022) 134975.
[41] D. Aslanidou, I. Karapanagiotis, C. Panayiotou, Tuning the wetting properties of siloxane-nanoparticle coatings to induce superhydrophobicity and superoleophobicity for stone protection, Mater. Des. 2016 (2018) 736–744.
[42] D. Aslanidou, I. Karapanagiotis, D. Lampakis, Waterborne superhydrophobic and superoleophobic coatings for the protection of marble and sandstone, Materials 11 (2018) 585.
[43] Y. Cao, A. Salvini, M. Camaiti, One-step fabrication of robust and durable superamphiphobic, self-cleaning surface for outdoor and in situ application on building substrates, J. Colloid Inter. Sci. 591 (2021) 239–252.
[44] P.N. Manoudis, Z. Chughtai, V. Tsiridis, S.P. Evgenidis, P.K. Spathis, T. D. Karapantsios, I. Karapanagiotis, Tuning the wettability of a commercial silane product to induce superamphiphobicity for stone protection, Coatings 13 (2023) 700.
[45] J. Jeevanandam, A. Barhoum, Y.S. Chan, A. Dufresne, M.K. Danquah, Review on nanoparticles and nanostructured materials: History, sources, toxicity and regulations, Beilstein J. Nanotechnol. 9 (2018) 1050–1074.
[46] M. Bundschuh, J. Filser, S. Lüderwald, M.S. McKee, G. Metreveli, G.E. Schaumann, R. Schulz, S. Wagner, Nanoparticles in the environment: where do we come from, where do we go to, Environ. Sci. Eur. 30 (2018) 6.
[47] A.B.D. Cassie, S. Baxter, Wettability of porous surfaces, Trans. Faraday Soc. 40 (1944) 546–951.
[48] P.N. Manoudis, I. Karapanagiotis, A. Tsakalof, I. Zuburtikudis, B. Kolinkeová, C. Panayiotou, Surface properties of superhydrophobic coatings for stone protection, J. Nano Res 8 (2009) 23–33.
[49] B.J. Basu, V.D. Kumar, Fabrication of superhydrophobic nanocomposite coatings using polytetrafluoroethylene and silica nanoparticles, ISRN Nanotechnol. (2011) 803910.
[50] T.M. Schutzius, I.S. Bayer, G.M. Jursich, A. Das, C.M. Megaridis, Superhydrophobic-superhydrophilic binary micropatterns by localized thermal treatment of polyhedral oligomeric silsesquioxane (POSS)—silica films, Nanoscale 4 (2012) 5378–5385.
[51] I. Karapanagiotis, D. Grosu, D. Aslanidou, K.E. Aifantis, Facile method to prepare superhydrophobic and water repellent cellulosic paper, J. Nanomater (2015) 219013.
[52] R.N. Wenzel, Resistance of solid surfaces to wetting by water, Eng. Chem. 28 (1936) 988–994.
[53] C.G.L. Furmidge, Studies at phase interfaces I. The sliding of liquid drops on solid surfaces and a theory for spray retention, J. Colloid Sci. 17 (1962) 309–324.
[54] W. Chen, A.Y. Fadeev, M.C. Hsieh, D. Oner, J. Youngblood, T.J. McCarthy, Ultrahydrophobic and ultralyophobic surfaces: some comments and examples, Langmuir 15 (1999) 3395–3399.
[55] E.A. Melo-Espinosa, Y. Sánchez-Borroto, M. Errasti, R. Piloto-Rodríguez, R. Sierens, J. Roger-Riba, A. Christopher-Hansen, Surface tension prediction of vegetable oils using artificial neural networks and multiple linear regression, Energy Proced. 57 (2014) 886–895.
[56] E. Chibowski, Surface free energy of a solid from contact angle hysteresis, Adv. Colloid Inter. 103 (2003) 149–172.
[57] K. Terpiłowski, D. Rymuszka, O.V. Goncharuk, I.Ya Sulymb, V.M. Gun'ko, Wettability of modified silica layers deposited on glass supportactivated by plasma, Appl. Surf. Sci. 353 (2015) 843–850.
[58] P.N. Manoudis, I. Zuburtikudis, G. Konstantopoulos, H.A. Khalifeh, C. Kottaridi, I. Karapanagiotis, Superhydrophobicity, photocatalytic self-cleaning and biocidal activity combined in a siloxane-ZnO composite for the protection of limestone, Biomimetics 9 (2024) 573.
[59] G. Vásquez, E. Alvarez, J.M. Navaza, Surface tension of alcohol + water from 20 to 50 °C, J. Chem. Eng. Data 40 (1995) 611–614.
[60] S.M.M. Ramos, J.F. Dias, B. Canut, Drop evaporation on superhydrophobic PTFE surfaces driven by contact line dynamics, J. Colloid Interface Sci. 44 (2015) 133–139.
[61] C. Li, Shujuan Liu, K. Yang, Z. Yuan, S. Meng, J. Du, X. Long, R. He, Q. Su, Preparation of superhydrophobic coatings on kraft paper for the protection of important documents, Colloids Surf. A 693 (2024) 134041.
[62] J.D. Rodrigues, A. Grossi, Indicators and ratings for the compatibility assessment of conservation actions, J. Cult. Herit. 8 (2007) 32–43.
[63] L. Dumée, J.L. Campbell, K. Sears, J. Schütz, N. Finn, M. Duke, S. Gray, The impact of hydrophobic coating on the performance of carbon nanotube bucky-paper membranes in membrane distillation, Desalination 283 (2011) 64–67.
[64] D. Kronlund, A. Bergbreiter, A. Meierjohann, L. Kronberg, M. Lindén, D. Grosso, J.-H. Smått, Hydrophobization of marble pore surfaces using a total immersion treatment method – product selection and optimization of concentration and treatment time, Prog. Org. Coat. 85 (2015) 159–167.
[65] M. Lettieri, M. Masieri, A. Morelli, M. Pipoli, A. Morelli, M. Frigione, Oleo/hydrophobic coatings containing nano-particles for the protection of stone materials having different porosity, Coatings 8 (2018) 429.
[66] E. Gkrava, V. Tsiridis, P. Manoudis, T. Zorba, E. Pavlidou, A. Konstantinidis, T. D. Karapantsios, P.K. Spathis, I. Karapanagiotis, A robust superhydrophobic coating of siloxane resin and hydrophobic calcium carbonate nanoparticles for limestone protection, Mater. Today Commun. 38 (2024) 108393.
[67] C. C. Gaylarde, Influence of environment on microbial colonization of historic stone buildings with emphasis on cyanobacteria, Heritage 3 (2020) 1469–1482.